

BBAMEM 75957

# Numerical analysis reveals complexities of glutamate transport

John F. Ash and Robert P. Igo, Jr.

*Department of Anatomy, School of Medicine, University of Utah, Salt Lake City, UT (USA)*

(Received 27 August 1992)

(Revised manuscript received 26 January 1993)

Key words: Glutamate transport; Kinetics; Curve fitting

The uptake of radiolabeled glutamate into cultured human (HeLa S<sub>3</sub>) and hamster (CHO-K1) cells was analyzed according to modified Michaelis-Menten models fit by the Marquardt least-squares method. Kinetic parameters not previously reported for these cells were obtained. Some rarely used features available with this fitting method proved to be extremely helpful. Most importantly, a goodness-of-fit measure revealed a significant alteration of glutamate uptake in HeLa cells that was induced by starvation. This apparent regulation, unexpected for glutamate transport, might have been missed if the fit had been judged by eye or by the magnitude of parameter standard deviations. Techniques for analyzing parameter distributions, improving experimental design and performing tests of significance are also described.

## Introduction

Several systems mediating transmembrane amino-acid fluxes in mammalian cells have been identified and defined by competition experiments [1]. An amino acid typically enters a cell via specific, saturable, high-affinity systems and also through one or more low affinity systems. Kinetic models for high-affinity transport are formally similar to the Michaelis-Menten model for enzyme catalysis [2]. The low-affinity flux is often modeled as a linear diffusion process, since it is difficult or impossible to saturate at reasonable substrate concentrations. Transport of a given substrate may thus be characterized by parameters  $V_{\max}$  and  $K_m$  for a high-affinity component and by a diffusion constant,  $k_D$ , summing low-affinity components [1,2]. Determining such parameters by statistical fitting, rather than by graphical techniques, has been advocated for at least 30 years [3,4]. The literature has addressed two major advantages of the statistical approach. First, it provides a method for calculating the precision of parameters, typically in the form of their standard deviations [3–6]. A second and related advantage is the ability, explicitly provided by some fitting procedures, to take measurement error into account during the process of parameter calculation [7]. Several fitting methods have been widely, but not universally, adopted.

We have initiated a study of glutamic acid uptake by the well known mammalian cell lines, HeLa S<sub>3</sub> and CHO-K1. Animal cells transport glutamate through a variety of saturable systems, with  $K_m$  values varying from micromolar to millimolar and with the import of glutamate being either linked or unlinked to the flow of other ions [8]. In human fibroblasts, for example, at least three saturable systems have been described: a sodium-independent glutamate and cystine transporter, system x<sub>c</sub><sup>-</sup>, with  $K_m \approx 300 \mu\text{M}$  [9], a sodium-dependent glutamate and aspartate transporter, system X<sub>AG</sub><sup>-</sup>, with  $K_m$  approx.  $20 \mu\text{M}$  [10] and a lower-affinity sodium-dependent system,  $K_m$  approx. 2 mM, thought to be the ASC transport system for neutral amino acids [10].

The results for HeLa and CHO cells reported here indicate that the complexity of glutamate transport may extend beyond the existence of several distinct saturable systems. We have observed that HeLa cells alter the kinetic profile of glutamate uptake in response to a one hour period of amino-acid deprivation and what at first appeared to be a single uptake system in CHO cells is likely the sum of two saturable systems. The process of identifying these complications forced us to learn about some less familiar features of curve-fitting. Although these features are not generally used by biochemists, as we illustrate here, they can be helpful. We have found, for instance, that a goodness-of-fit measure should be routinely checked. This alerts one to the possibility that the model equation being fit is wrong even if the fit appears good on a graph. As a caution, however, we will show that an acceptable

Correspondence to: J.F. Ash, Department of Anatomy, University of Utah, Salt Lake City, UT 84132, USA.

goodness-of-fit value does not guarantee a correct model. A second feature worth noting when fitting nonlinear models is that the standard deviation estimates calculated by the fitting program can be untrustworthy; it is possible for parameters not to be distributed normally, i.e., not in a 'bell-shaped' curve. One can test for and, if necessary, overcome this problem using Monte Carlo simulation to determine parameter confidence limits directly. In either case, it is possible to test the significance of differences between parameters determined under two conditions. Finally, curve-fitting programs can help improve experimental design rapidly and easily. These procedures do not replace the experience and insight required to create a useful kinetic model or the necessity to make careful experimental measurements. They do, however, provide some straightforward mathematical tools for testing important features of a model once good data are obtained.

## Materials and Methods

L-Glutamic acid and other chemicals were purchased from Sigma (St. Louis, MO, USA) unless otherwise noted. L-[<sup>3</sup>H]Glutamate was obtained from Amersham International (Arlington Heights, IL, USA).

The human carcinoma cell line, HeLa S<sub>3</sub> [11], was obtained from Melvin Simon, University of California at San Diego in 1979. A randomly isolated subclone of these cells, HC-4 [12], was used for all studies reported here. The Chinese hamster ovary cell line, CHO-K1, was obtained from the American Type Culture Collection (Rockville, MD, USA). Cells were maintained on Costar dishes (Cambridge, MA, USA) in D/F H5C5 medium: 45% Dulbecco's modified Eagle medium, 45% Ham F12 medium, 5% horse serum (Hyclone, Logan, UT, USA), 5% calf serum (Hyclone), 100 U/ml penicillin, 100 µg/ml streptomycin and 2.45 g/l NaHCO<sub>3</sub>.

Uptake of radiolabeled L-glutamate was measured using cells grown on 24-well cluster dishes (Costar) essentially as described by Gazzola et al. [13] with modifications developed in our laboratory (DeBusk, W.E. and Ash, J.F., data not shown). Cells were cultured for 24 h before assay and were subconfluent at that time. Dishes were rinsed twice with HBS · MCD (137 mM NaCl, 0.7 mM K<sub>2</sub>HPO<sub>4</sub>, 10 mM Hepes (Research Organics, Cleveland, OH, USA), 1 mM MgCl<sub>2</sub>, 1 mM CaCl<sub>2</sub>, 1 g D-glucose/liter (pH 7.4) at 37°C, adjusted with KOH) or HBC · MCD (137 mM choline chloride replacing NaCl in HBS · MCD) before uptake was initiated by addition of [<sup>3</sup>H]glutamate (5 µCi/ml) in the same type of saline used for prerinsing. After 2 min at 37°C, during which period velocity remained constant, the radioactive solutions were shaken out and the dishes rinsed four times with ice-cold PBS (0.15 M NaCl, 10 mM K<sub>2</sub>HPO<sub>4</sub> (pH 7.4) at

20°C). Cell-associated [<sup>3</sup>H]glutamate was extracted with 10% trichloroacetic acid and radioactivity determined with a Packard Instruments (Downers Grove, IL, USA) 2000CA liquid scintillation counter. The protein in each well was determined by the bicinchoninic acid method [14] using reagents from Pierce (Rockford, IL, USA). Velocities (nmol glutamate/mg cell protein per min) and their standard deviations were obtained from the average of three wells and 8 to 16 glutamate concentrations were analyzed per experiment.

Velocity data were initially fit to the Michaelis-Menten equation plus a non-saturable term,  $k_D$ :  $V = V_{\max}[S]/(K_m + [S]) + k_D[S]$ . The Marquardt least-squares method was used [15] as implemented by the Macintosh program KaleidaGraph (Synergy Software, Reading, PA, USA) or by our own code written in the C programming language and employing the programs *mrqmin* and *mrqcof* of Press et al. [16]. KaleidaGraph was used to prepare the figures. Parameter values calculated by the programs are reported  $\pm 1$  S.D. Parameter units were:  $K_m$ , µM;  $V_{\max}$ , nmol glutamate/mg protein per min;  $k_D$ , pmol glutamate/mg protein per min per µM glutamate. Both fitting implementations modified the Marquardt method by minimizing the  $\chi^2$  statistic. In this case,  $\chi^2 = \sum_{i=1}^n ((\dot{v}_i - V_i)/s_i)^2$  for  $n$  substrate concentrations,  $\dot{v}_i$  is the  $i$ th measured average velocity,  $s_i$  is the standard deviation of  $\dot{v}_i$  and  $V_i$  is the corresponding velocity calculated from the model equation. The final  $\chi^2$  value returned by these programs can be converted into a measure of the goodness-of-fit: the probability that the measured velocities come from a process described by the model equation using the calculated parameters. Following the convention of Press et al. [16], this probability will be called  $q$ . The final  $\chi^2$  can be converted into probability  $q$  by numerical calculation or estimated from published tables of  $\chi^2_{df}$  where  $df$  is the degrees of freedom, here the number of substrate concentrations minus the number of parameters fit. We used function *gammq* [16], which employs the appropriate incomplete gamma function, to calculate  $q$ . For the conversion of  $\chi^2$  to  $q$  to be meaningful, velocity measurements must be normally distributed, and this can be analyzed with the  $W$ -test [17]. This is a general test of a distribution's normality and Royston has developed an algorithm for calculating the  $W$  statistic for sample sizes 3 to 2000 [18]. We translated Royston's Fortran programs directly into the C language and used them to calculate  $W$  and the significance statistic,  $pW$ , the probability that a given set of values was normally distributed.

Monte Carlo simulation of these experiments assumed: (1) that the sets of velocity measurements  $\{\dot{v}_i\}$  at each substrate concentration were normally distributed and (2) that the ratio  $r_i$  of the sample standard deviation of  $\{\dot{v}_i\}$  to the mean of  $\{\dot{v}_i\}$ ,  $r_i = s_i/\dot{v}_i$ , would remain constant from trial to trial. This proce-

ture simply provides a method for simulating repetitions of the experiment with a computer program by assuming that random normal measurement error would provide the only differences among a set of experiments. The program was supplied with initial data:  $[S]_i$ ,  $\dot{v}_i$  and  $s_i$ . The Box-Muller method [16] was used to obtain a random unit normal deviate,  $\delta_i$ , for each velocity: this is a sample from a random variable which is normally distributed with mean 0 and standard deviation 1. A new set of simulated average velocities and standard deviations,  $\dot{v}_i^*$  and  $s_i^*$ , were then produced:  $\dot{v}_i^* = \dot{v}_i + s_i \cdot \delta_i$ ,  $s_i^* = r_i \cdot \dot{v}_i^*$ . These simulated data were fit to the appropriate model and the trial's parameter values listed. This process was repeated up to 10000 times and each parameter's average and standard deviation were calculated and compared with the estimates provided by the Marquardt method for the original data. The first 2000 parameter values were analyzed by the  $W$ -test and the probability,  $pW$ , that they were normally distributed was calculated. Listings of our programs in C are available upon request.

Depending on which starting velocity values are supplied to the program, two different types of simulation can be performed. To test how experiments fit to a particular model equation behave given the observed measurement errors, one begins with the actual measured mean velocities,  $\dot{v}_i$ , simulates many experiments, and asks if the fitted parameter values cluster together upon repetition. If this 'data-based' simulation reveals that a parameter's value varies widely upon repetition then a different model or altered protocol may be indicated. Alternatively, if it is considered adequate

and stable then the model can be used to calculate an 'ideal' velocity at each substrate concentration to generate the starting velocities [19]. The list of parameter values obtained by this 'model-based' simulation then represents the best estimate of the distribution that would be expected for actual experimental repetitions. If this list is placed in numerical order it can directly provide confidence limits for a parameter. These confidence limits can be used to describe parameters which are not distributed normally. For fits of experiments associated with high  $q$  probabilities, the difference between data-based and model-based simulations will be slight.

## Results

A typical analysis of glutamate uptake by HeLa cells in sodium-containing saline is shown in Fig. 1A. As expected, uptake is mediated by at least two processes: one saturable (hyperbolic), dominating at low substrate concentrations, and an apparently non-saturable, linear process evident at higher concentrations. Velocity measurements were analyzed by the  $W$ -test and found to be distributed normally ( $pW > 0.05$ ). As seen in Fig. 1B, the standard reciprocal transformation of an Eadie-Hofstee plot does not yield a straight line because of the contribution of the linear process.

The curve determined by the Marquardt method in Fig. 1A is associated with Michaelis-Menten parameters  $K_m = 61 \pm 8$  and  $V_{\max} = 2.1 \pm 0.2$ , and linear parameter  $k_D = 3.9 \pm 0.2$ . Since the  $W$ -test revealed that velocity measurements were normally distributed, the

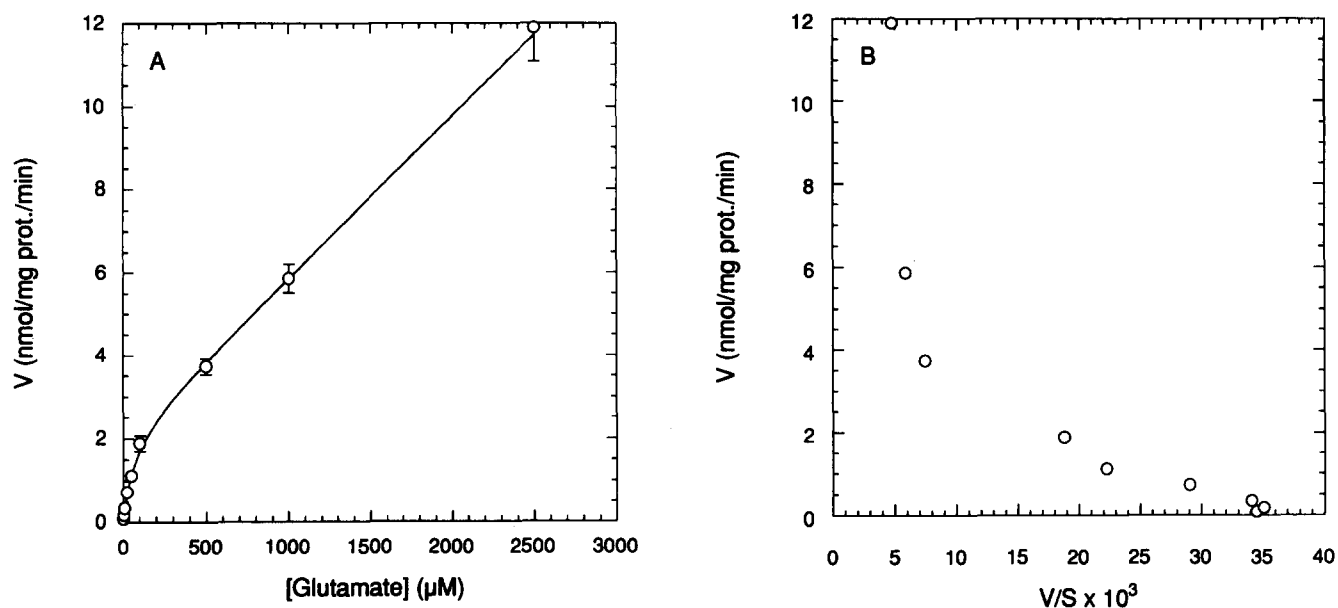


Fig. 1. Glutamate uptake by HeLa cells measured in HBS-MCD immediately after rinsing growth medium from cells. (A) Velocities are shown  $\pm 1$  S.D. (when larger than the symbol). The experiment included measurements at 5 and 10 mM glutamate which are not shown so that the saturable uptake at low concentrations can be seen. The data were fit to  $V = V_{\max}[S]/(K_m + [S]) + k_d[S]$  using the Marquardt method. (B) An Eadie-Hofstee plot of the data from (A).

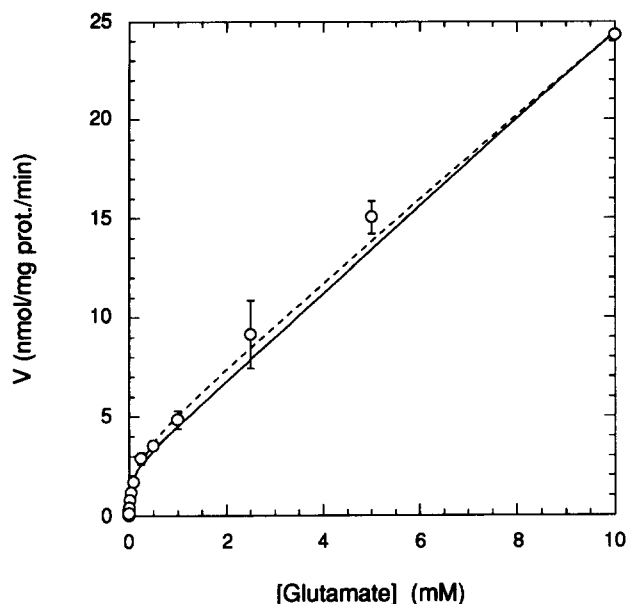


Fig. 2. Glutamate uptake by starved HeLa cells. Cells were incubated for 1 h in HBS·MCD before uptake. The data were fit to the same equation as used in Fig. 1A (solid curve) or to  $V = V_{\max 1}[S]/(K_{m1} + [S]) + V_{\max 2}[S]/(K_{m2} + [S]) + k_d[S]$  (dashed curve).

$\chi^2 = 5.8$  could be converted into probability  $q = 0.66$ . This high probability suggests that it is reasonable to assume that the data of Fig. 1A could come from a process defined by these parameters. This and all other experiments described here were repeated at least

once with no significant differences observed in the parameter values and the results of experiments with the best  $q$  value were reported.

In Fig. 2, glutamate uptake by HeLa cells was measured after the cells were incubated for 1 h in HBS·MCD. The incubation in saline before assay reduces the internal amino-acid pools and should reveal if uptake is being driven by exchange for internal substrates [2]. In Fig. 2, the data were first fit to the same equation as for Fig. 1A (solid curve) yielding  $K_m = 49 \pm 2$ ,  $V_{\max} = 2.3 \pm 0.1$ ,  $k_D = 2.2 \pm 0.0$ . Comparing these results with those of Fig. 1A, without saline preincubation, it would appear that this treatment had little effect on uptake: a minor decrease in  $K_m$  and a 40% reduction in uptake through the non-saturable system. However, the  $\chi^2$  for this fit was 53.2,  $q < 10^{-6}$ . This low probability suggested that the model being fit was incorrect and the values calculated for the parameters should not be taken seriously. As judged by eye, the fit is not as good as that of Fig. 1A, but it appears to be reasonable. Repetitions of the experiment, however, continued to yield unlikely  $q$  values (data not shown).

We explored other models and found that if the data were fit to a two saturable and one linear system model (Fig. 2, dashed curve) a  $\chi^2$  of 8.2 and  $q$  value of 0.51 were obtained. The fit was visually only slightly better but now statistically believable. The five parameters for the two-system fit were:  $K_{m1} = 19 \pm 6$ ,  $V_{\max 1} =$

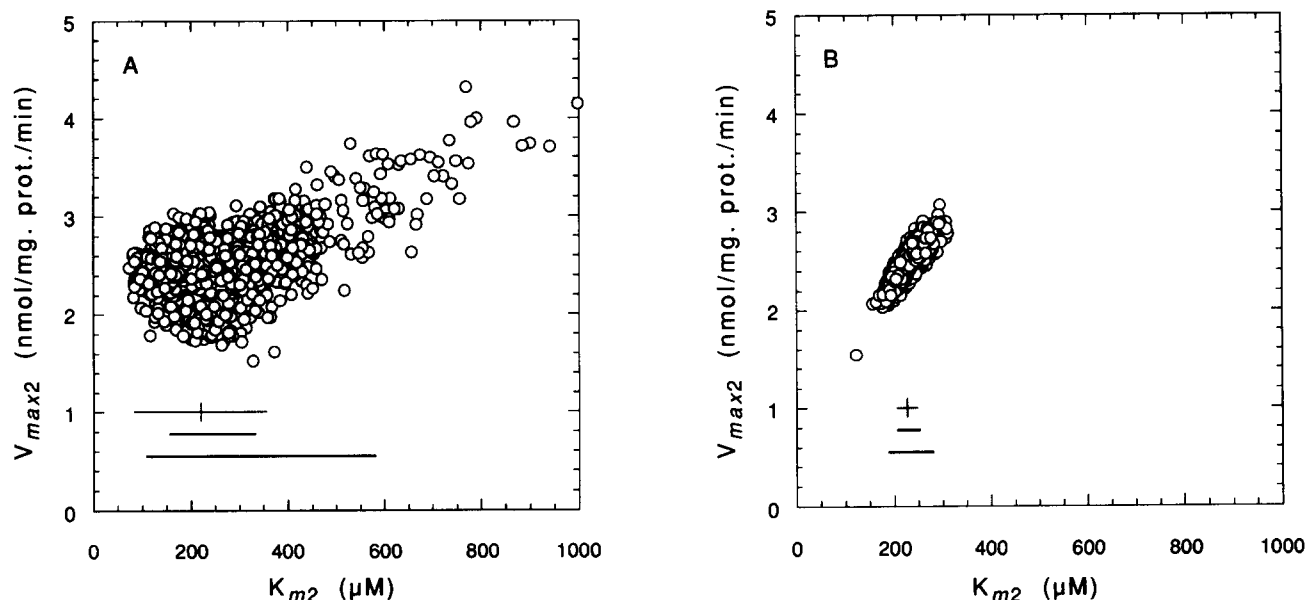


Fig. 3. Parameter codistributions from Monte Carlo simulations. The parameters calculated from the data for the model of Fig. 2B were used as the basis for 2000 Monte Carlo simulations. (A) The codistribution of  $V_{\max 2}$  and  $K_{m2}$  illustrates the nonnormal distribution of these parameters. The thin horizontal bar under the distribution indicates one standard deviation above and below  $K_{m2}$  (vertical line) calculated from the original data by the Marquardt method. The thick bar below that indicates the 68.3% confidence limits for the 2000 points shown. It is shifted to the right relative to the standard deviation estimate. The bottom bar indicates the 95% confidence limits of the 2000 points. This would represent approx.  $\pm 2$  S.D. of a normal distribution:  $K_{m2}$  is strongly positively skewed. (B) When the other parameters were fixed and only  $V_{\max 2}$  and  $K_{m2}$  were fit, their codistribution from 2000 simulations is more compact and symmetric; the bars below the distribution represent the same quantities as in (A).

$0.85 \pm 0.38$ ,  $K_{m2} = 220 \pm 136$ ,  $V_{max2} = 2.4 \pm 0.2$  and  $k_D = 2.1 \pm 0.0$ . If the data of Fig. 1A are fit to a model combining two saturable systems, one obtains the original saturable parameters for one of the systems and unlikely values with very large standard deviations for the second system.

We investigated the large standard deviations reported for the parameters determined in Fig. 2B using Monte Carlo simulation. An analysis of 2000 simulated trials, either data- or model-based, revealed that none of the five parameters was distributed normally ( $pW < 10^{-6}$ ). For example, the one standard deviation confidence limits for  $K_{m2}$  calculated by the Marquardt method would be 84 to 356 ( $K_{m2} = 220 \pm 136$ ). The 68.3% limits from the 2000 model-based simulated trials were 157 to 331 ( $\pm$  one standard deviation contains 68.3% of the area under a normal distribution). This can be seen in Fig. 3A, which shows the codistribution of  $V_{max2}$  and  $K_{m2}$ . Thus, given reasonable and normally distributed measurement error, Monte Carlo simulations of this experiment generate highly positively skewed values for  $K_{m2}$ . The standard deviation estimate provided by the Marquardt method is not useful in this case because it does not properly describe the expected distribution of the parameter.

The large uncertainties associated with the determination of  $K_{m2}$  in this case are a feature of fitting a two-saturable system model and not a function, for example, of large measurement errors. If, however, the values for  $K_{m1}$ ,  $V_{max1}$ , and  $k_D$  listed above are kept

fixed and the data of Fig. 2B fit only for  $K_{m2}$  and  $V_{max2}$  the results are:  $K_{m2} = 227 \pm 21$ ,  $V_{max2} = 2.5 \pm 0.1$ ,  $\chi^2 = 8.4$ ,  $q = 0.75$ . The probability for this fit is higher because of the increased degrees of freedom. This situation was analyzed by another 2000 simulations. In this case, the parameters were normally distributed, as judged by the  $W$ -test ( $pW > 0.05$ ). As seen in Fig. 3B, the Marquardt standard deviation estimate for  $K_{m2}$  is virtually identical to the 68.3% confidence interval provided by the simulation. In this case the Marquardt method's standard deviation estimate is useful. The Marquardt algorithm has particular trouble finding  $K_{m2}$  in cases where two saturable systems are combined with a non-saturable process, as in Fig. 3A. When only the two parameters were fit (Fig. 3B), the codistribution was more symmetric and compact with only one obvious outlier.

Holding the values of three parameters constant was a convenient means of demonstrating the variable behavior of the Marquardt algorithm with regard to standard deviation calculations. Arbitrarily fixing a subset of parameter values determined from a single experiment in order to improve the estimation of the remainder by recalculation is not mathematically justified. Experimental conditions, such as the use of an inhibitor specific for one system would have to be discovered to allow independent determination, for instance, of  $K_{m1}$ ,  $V_{max1}$ . It appears that *N*-methyl-2-aminoisobutyric acid (MeAIB), a substrate of amino-acid transport system A [1], is a competitive inhibitor

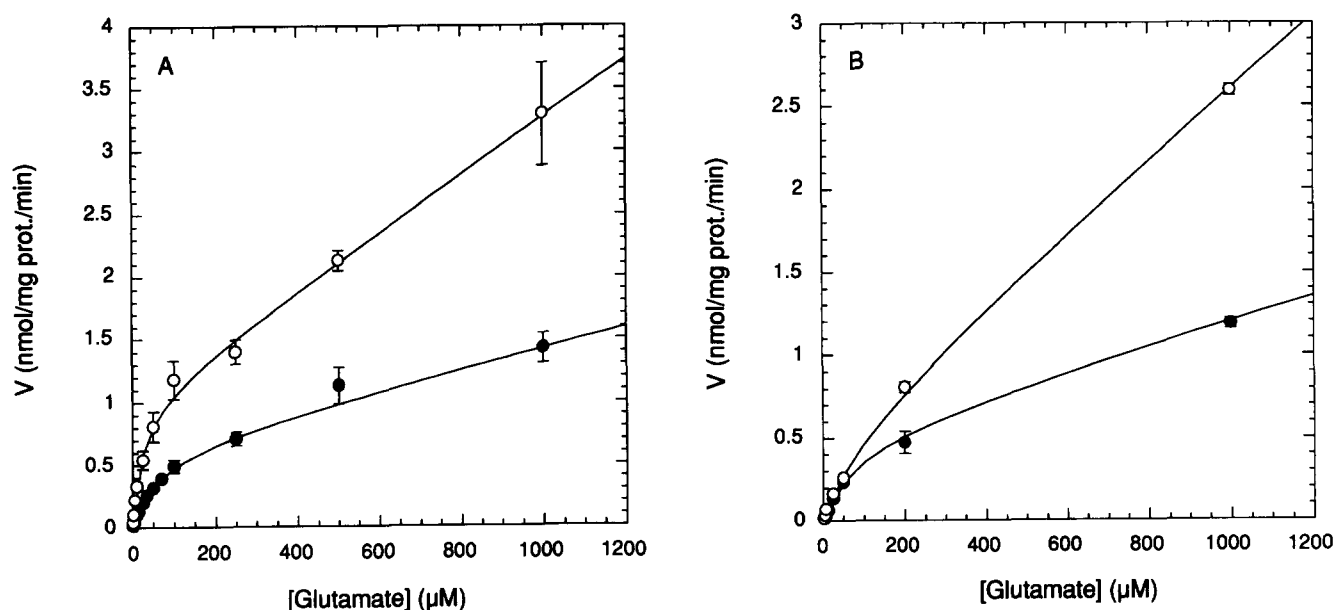


Fig. 4. Glutamate uptake by CHO cells without preincubation in saline. (A) Upper curve ( $\circ$ ) shows the results of measurements made in HBS·MCD fit to the equation of Fig. 1A. No significant difference was seen when the cells were preincubated in this saline for one hour before assay (not shown). When the assay is performed without sodium ions ( $\bullet$ ), i.e., in HBC·MCD,  $K_m$  is increased and  $V_{max}$  and  $k_d$  are decreased. Additional velocities determined at 2.5, 5.0 and 10.0 mM were not shown here, but used for parameter calculations. (B) Glutamate uptake was measured in the presence of 1.0 mM aspartate with ( $\circ$ ) and without ( $\bullet$ ) sodium and fit as for (A). An additional measurement at 5.0 mM is not shown, in order to emphasize the low velocity data.

of the lower-affinity system 2 defined by  $K_{m2}$ : when uptake by starved HeLa cells was measured in the presence of 10 mM MeAIB,  $K_{m1}$  and  $V_{max1}$  were not affected. When all five parameters were fit,  $K_{m2}$  was increased to  $1290 \pm 929$ , and holding three parameters constant, as described above, yielded  $K_{m2} = 1400 \pm 260$ . This result supports fixing the values of the high affinity, system 1, parameters and recalculating values for system 2 as described above for the noninhibited case. MeAIB had no effect on the uptake of glutamate by nonstarved cells (results not shown). The original question – whether the transport seen in Fig. 1 was driven by exchange – cannot as yet be answered because the starvation treatment produced such a dramatic alteration in uptake.

The uptake of glutamate by CHO cells was analyzed by the experiments of Fig. 4. The upper curve (Fig. 4A) shows that uptake measured in HBS · MCD can be fit with a one saturable, one non-saturable system model. The parameters for this fit are:  $K_m = 24 \pm 3$ ,  $V_{max} = 1.05 \pm 0.09$ ,  $k_D = 2.2 \pm 0.1$ ,  $\chi^2 = 4.3$ ,  $q = 0.96$ . 1 h preincubation in HBS · MCD had no significant effect on these parameters, unlike the case seen for HeLa cells (Fig. 2). Given the apparent stability of the saturable system's parameters to starvation and the high probability associated with the fit, one could conclude that CHO cells contain a single high-affinity saturable glutamate-uptake system.

When glutamate uptake by CHO cells was measured under other conditions a more complex situation was found. All parameters were affected when measured in sodium free saline, HBC · MCD, Fig 4A lower curve:  $K_m = 62 \pm 3$ ,  $V_{max} = 0.62 \pm 0.03$ ,  $k_D = 0.87 \pm 0.01$ ,  $\chi^2 = 3.79$ ,  $q = 0.98$ . Replications of this experiment resulted in data which, when fit to the same equation, resulted in similar parameter values but with  $q$  values as low as 0.001. The lower probabilities were associated with more precise velocity determinations: it appeared that the model was not adequate for uptake measured in the absence of sodium, but recognizing this required small velocity standard deviations. When analyzed in the presence of 1 mM aspartate, saturable glutamate uptake was independent of extracellular sodium (Fig. 4B). A single saturable system was found in the sodium free, 1 mM aspartate condition with  $K_m = 84 \pm 13$ ,  $V_{max} = 0.51 \pm 0.08$ ,  $k_D = 0.7 \pm 0.1$ ,  $\chi^2 = 8.6$ ,  $q = 0.12$ . In the presence of sodium, 1 mM aspartate produced essentially the same saturable profile:  $K_m = 97 \pm 16$ ,  $V_{max} = 0.49 \pm 0.08$ , with  $k_D = 2.2 \pm 0.1$ ,  $\chi^2 = 8.9$ ,  $q = 0.11$ . We assume that these results are due to the presence of two saturable systems for glutamate import in CHO cells. One is sodium independent, insensitive to aspartate, with an apparent  $K_m$  of approx. 90. The other saturable system is partially sodium dependent, inhibited by aspartate, with a  $K_m$  of approx. 20 in HBS · MCD as deduced by fitting the data

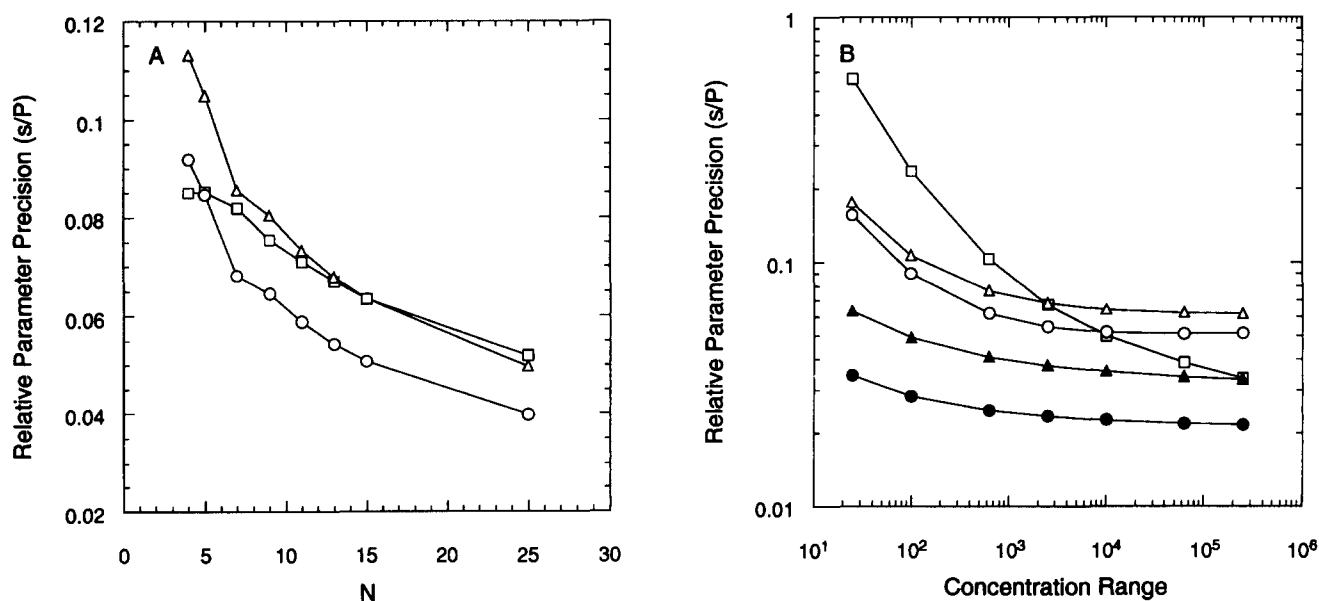


Fig. 5. Optimizing parameter precision. A hypothetical Michaelis-Menten process ( $V_{max} = 1.0$ ,  $K_m = 25.0$ ), with (open symbols) or without (closed symbols) a non-saturable process ( $k_d = 2.0$ ), was used to calculate velocities to be fit by the Marquardt method, assuming a relative velocity standard deviation of 0.05. Symbols:  $V_{max}$  ( $\circ$ );  $K_m$  ( $\Delta$ ) and  $k_d$  ( $\square$ ). Points are connected by lines. (A) With concentrations spread geometrically over a 2500-fold range (50-fold above and below  $K_m$ ), relative parameter precisions,  $s/P$  ( $P$  = fitted parameter value,  $s$  = standard deviation of  $P$ ), were calculated as a function of  $n$ , the number of concentrations. (B) With  $n = 13$ , concentrations were geometrically spaced across the indicated range (e.g.,  $1/5 \cdot K_m$  to  $5 \cdot K_m$  for range = 25) and relative parameter precisions were calculated.

of Fig 4A for two saturable systems. The non-saturable uptake of glutamate in CHO cells was not inhibited by 1 mM aspartate, but was partially dependent on sodium. It is the likely presence of two saturable systems in sodium-free saline, one with greatly reduced velocity, which complicated fitting the data to a single saturable system model. Further analysis of these systems will be reported elsewhere (Igo, R.P., Jr. and Ash, J.F., data not shown). Of interest here is the fact that the Marquardt algorithm did not signal by a low  $q$  value the likely existence of alternate models for the data of Fig. 4A. Two systems with similar values for  $V_{\max}$  and  $K_m$  may appear as one to the Marquardt algorithm. If the data of Fig. 4A are fit to a model combining two saturable systems one obtains the same result as for nonstarved HeLa: the original saturable parameters for one of the systems and unlikely values for the second system.

Finally, we considered the general question: how does experimental design affect the parameter precision, as measured by standard deviation? This is controlled, in part, by the number of concentrations used ( $n$ ). Fig. 5A shows the analysis of a hypothetical Michaelis-Menten process,  $K_m = 25$ ,  $V_{\max} = 1.0$ , with a non-saturable component,  $k_D = 2.0$ . A relative standard deviation,  $r = 0.05$ , was assumed for each velocity value computed. Monte Carlo simulation revealed that all parameters were normally distributed and that the standard deviation estimates of the Marquardt method were accurate. With concentrations were spread geometrically over a 2500-fold range (50-fold above and below  $K_m$ ), precisions of  $K_m$  and  $V_{\max}$  improved rapidly as  $n$  increased to 7 and more slowly for all three parameters after that.

The relationship of parameter precision to the distribution of concentrations is more complex. Fig. 5B relates relative parameter precision to the concentration range, beginning at 25-fold (5-fold above and below  $K_m$ ). 13 concentrations were geometrically spaced across each range. For a simple Michaelis-Menten process (filled symbols) precisions of  $V_{\max}$  and  $K_m$  were different, but each improved as the range increased. When the non-saturable component was added (open symbols), its precision improved as the concentration range increased, but precisions of  $V_{\max}$  and  $K_m$  were optimal only near the 2500-fold range and began to worsen slowly with increasing spread. Parameter precision is directly related to relative velocity measurement error: reducing  $r$  from 5% to 2.5% halved the standard deviations of  $V_{\max}$ ,  $K_m$  and  $k_D$ . We have empirically determined that, when a non-saturable component is involved, a non-uniform spacing of concentrations about  $K_m$  can improve precision of all three parameters. The majority of concentrations should be geometrically spaced within 10- to 20-fold

below and above  $K_m$  and additional higher concentrations are used to improve estimation of  $k_D$ .

## Discussion

A statistical fitting method specifically benefits analysis of amino-acid transport experiments because it can accommodate the significant non-saturable uptake typically encountered. One could attempt to fit the low-velocity points in the Eadie-Hofstee plot of Fig. 1B with a straight line and obtain the Michaelis-Menten parameters, but this adds complications which the reciprocal analysis was designed to avoid. A fitting algorithm can utilize all the data to determine parameter values. The Marquardt method has long been employed for analysis of transport parameters [20,21] and, when formulated to minimize  $\chi^2$ , it offers a simpler method for including actual measurement errors in parameter calculations than provided by some other kinetic analysis programs [7]. The Marquardt method is one of several iterative techniques used to perform nonlinear regression. It is efficient and avoids potential problems encountered by other algorithms. A useful discussion of this and other considerations relevant for nonlinear model analysis is provided by Motulsky and Ransnas [19].

Determining the goodness-of-fit has not been common practice in kinetic studies. The usefulness of calculating  $q$  was demonstrated by the alert it generated for the analysis of glutamate uptake by HeLa cells seen after starvation in Fig. 2. One could have compared the results of Fig. 2 with Fig. 1A, assumed that the saline incubation had a secondary effect on the experiment – increasing scatter and making the fit appear less good – and concluded that starvation changed the original parameters only slightly. However, finding  $q < 10^{-6}$  for a single saturable process forced us to consider this result in more detail. As mentioned above, the existence of two constitutively expressed saturable glutamate uptake systems, for instance  $X_{AG}^-$  and  $x_c^-$  [10], has been observed in other cells, although often only one system is present [8,9]. A regulatory event converting an apparent single system to two systems, however, has not been reported and was unexpected. We did not, for instance, observe an alteration in the behavior of CHO cells after starvation. It is not yet clear that either of the systems observed in starved HeLa cells corresponds to any of those described in other cells, or that they are directly related to the single system initially present in nonstarved cells. The appearance of system 2 with a high  $K_m$  in response to low substrate concentrations would not seem to benefit a cell, and, in fact, this system may function primarily in some other capacity. On the other hand, the ability to activate rapidly high-affinity system 1 could be important for

cells faced with declining glutamate levels. The  $K_m$  of system 1 in HeLa (about 20  $\mu\text{M}$ ) is very similar to that of system  $X_{AG}^-$  in human fibroblasts [10], but regulations of the fibroblast system have not been described. The inhibition of system 2 by MeAIB suggests that it may be related to amino-acid transport system A [1]. However, the apparent  $K_i$  for MeAIB inhibition of glutamate uptake by system 2 is about 2 mM, as deduced by the six-fold increase in  $K_{m2}$  produced by 10 mM MeAIB. The  $K_i$  for MeAIB inhibition of system A in other cells is about 300  $\mu\text{M}$  [22], however, so it is not certain that this system is identical with system A. The large standard deviations associated with simultaneously fitting two saturable systems would not allow us to conclude that  $K_i$  is significantly different from 300  $\mu\text{M}$ . When we fixed the values for the high-affinity system and the non-saturable process, the increase in  $K_{m2}$  produced by MeAIB is significant, suggesting, at least, that MeAIB is a competitive inhibitor of system 2. Further studies will be required to determine, for instance, if two systems are present before starvation and are modified during saline incubation, or if previously silent systems are activated. In either case, this dramatic alteration of glutamate uptake is intriguing and could have special significance for nervous system function [23].

It is suggested that publishing a goodness-of-fit statistic along with parameters and standard deviations, or mentioning that all fits have been judged to be acceptable, would be a useful practice. Other methods for analyzing goodness-of-fit have been proposed. Analyzing the relative size of parameter standard deviations [24] would not seem to be reliable in all cases: for instance, it was no help in the experiments of Fig. 2. Our experience with modeling kinetic data suggests that parameter standard deviations, as calculated by the Marquardt method, can depend more on the size of the standard deviations of the experimental data than on the goodness-of-fit. Mannervik has described a method [25], based on analyzing the distribution of residuals, for examining goodness-of-fit and identifying systematic errors. This method is, however, more complicated than converting  $\chi^2$  to  $q$  and may not be as easily susceptible to automatic computation. Mannervik also described a test for comparing two models, which would be useful, for instance, after a low  $q$  value has signaled a problem with the initial model chosen. Converting  $\chi^2$  to  $q$  assumes that measurement errors are normally distributed, which can be checked with the  $W$ -test. In cases where these errors are not normally distributed outlier points may be more numerous and a different fitting method should be considered [26].

There is no firm rule for deciding if a particular goodness-of-fit is acceptable. Press et al. [16], who provide a lucid and entertaining discussion of this

issue, suggest that, in general,  $q > 0.1$  is a reasonable level for accepting a model, although in some cases models with  $q > 10^{-3}$  may be acceptable if alternative models are much less likely. A single outlying data point with a small standard deviation can have a dramatic effect on  $q$ . Repetitions of the experiment and familiarity with the system will provide guides for establishing reasonable significance levels. In any case, being forced to consider the goodness-of-fit objectively is clearly superior to judging a graph by eye.

The Marquardt method did not distinguish between a single saturable process and two saturable processes with similar  $K_m$  and  $V_{\max}$  values that appear to exist in CHO cells. This failure to alert us to a problem with our initial model for analyzing the data of Fig. 4 cautions that an acceptable goodness-of-fit is not sufficient to prove a model. It appears that CHO cells contain glutamate transport systems resembling both  $X_{AG}^-$  and  $x_c^-$  [8–10], although more work will be required to describe completely the nature of the systems present in CHO and compare them with those defined in other cells. The numerical differences between the kinetic parameters of systems  $X_{AG}^-$  and  $x_c^-$  in human fibroblasts were sufficiently large that it was obvious that both of these high-affinity systems were present [10]. This was not the case in CHO cells. Clearly, there may be several reasonable but distinct models available for any process under study. Given precise data, some models can be rejected if they yield unlikely fits. Additional experimental strategies must be discovered to decide among different, but statistically adequate, models.

It is possible to test the significance of differences between parameters determined by independent measurements. For normally distributed parameters, the logic of this test is similar to that used when testing the significance of differences between means of two sets of measurements. Consider the results of Fig. 4B, where the  $K_m$  values for CHO cells were determined with and without sodium ( $97 \pm 13$  vs.  $84 \pm 16$ ) – are these different? Monte Carlo simulations found that these parameters were normally distributed. One assumes that a large number of experiments performed with and without sodium would produce normal parameter distributions, with  $\theta_A$  the true mean of the distribution of  $K_m$  measured in sodium and  $\theta_B$  the true mean measured without sodium. The null hypothesis is  $\theta_A = \theta_B$ , or these distributions are the same. If unbiased samples ( $K_{mA} \pm s_A$ ,  $K_{mB} \pm s_B$ ) are taken from these distributions then  $(K_{mA} - K_{mB} - (\theta_A - \theta_B)) / \sqrt{s_A^2 + s_B^2}$  will have a standard normal distribution: mean 0 and standard deviation 1. One can test the null hypothesis by determining if a specified interval about the difference between a given pair of parameters,  $K_{mA} - K_{mB}$ , includes 0. A commonly chosen interval is



$\pm 1.96\sqrt{s_A^2 + s_B^2}$  which contains 95% of the area under the standard normal distribution. If  $\theta_A = \theta_B$  then 0 will lie outside the interval  $(K_{mA} - K_{mB}) \pm 1.96\sqrt{s_A^2 + s_B^2}$  by chance only 5% of the time. For the data of Fig. 4B,  $K_{mA} - K_{mB} = 97 - 84 = 13$  and  $1.96\sqrt{s_A^2 + s_B^2} = 1.96\sqrt{13^2 + 16^2} = 40$ . Since 0 is within the 95% interval,  $13 \pm 40$ , the null hypothesis is not rejected. We cannot conclude that the parameters are different: sodium has no effect on the  $K_m$  of the saturable system seen in the experiment of Fig. 4B at the 0.05 level of significance.

The possibility that parameters are not always distributed normally, as seen for starved HeLa cells in Fig. 3, suggests that Monte Carlo simulation of a process under study should be performed to validate the use of the test of significance described above. In those cases where parameters are not normally distributed, as in Fig 3A, simulations themselves must be used to test if parameters from two measurements differ. One conducts  $n$  independent model-driven simulations of the process using parameters determined under conditions A and B and generates two lists for each parameter,  $(P_A)$  and  $(P_B)$ . Next, a difference distribution of  $n$  elements is constructed:  $\{P_{A1} - P_{B1}, P_{A2} - P_{B2}, \dots, P_{An} - P_{Bn}\}$ . One can then order and examine this distribution to determine directly if 0 is within its central 95% to test the null hypothesis at the 0.05 level. Monte Carlo simulation provides a description of the model's behavior under a relevant set of experimental conditions and can provide confidence intervals and significance testing where required.

An analysis of experimental design (Fig. 5) aimed at improving parameter precision produced useful though surprising results. Given an initial estimate of parameter values and individual measurement errors, one can quickly determine how the number and distribution of points will affect a parameter's precision. From a practical standpoint, for our measurements of a saturable plus non-saturable system there is relatively little gain in precision realized by increasing the number of substrate concentrations above 10, and it appears that the Marquardt algorithm operates best if the concentrations are varied in an asymmetric manner: about 20-fold on either side of the  $K_m$  in a geometric interval plus additional high concentrations up to 50-fold above  $K_m$  which improve estimation of  $k_D$ . Utilizing such a wide substrate range may seem unusual because it is often assumed that substrate concentrations kept within five-fold of  $K_m$  are optimal for kinetic analysis of enzymes in solution [5,24,27]. This assumption is likely based, in part, on studies of spectroscopic determination of the dissociation (equilibrium) constant,  $K$ , describing intramolecular complexes in solution. Analyses by propagation of errors and information theory demonstrated that the most efficient ligand concentra-

tions for such determinations are those that keep the saturation fraction of the most dilute component between 0.2 and 0.8 and, on the practical side, measurement error often increases significantly at concentrations beyond those values [28,29]. Assuming that these analyses can be extended to transport kinetics, one may first note that velocity errors do not necessarily increase rapidly beyond a five-fold range of  $K_m$ . Second, when studying transport with whole cells, several systems, including very low-affinity, 'non-saturable' ones, are usually involved. A wide range of substrates must then be employed with least-squares analysis to optimize parameter determinations, as demonstrated in Fig. 5B. The choice of the substrate range will depend on the model and requires some trial and error to determine. Similarly, it was recommended that determinations of models and dissociation constants for systems of multiple equilibria should include 75% of the entire saturation range [30]. A different approach for estimating kinetic parameters of proven models has been proposed and is based on algebraic solution of simultaneous equations [25,31,32]. By this method, velocities are determined at a minimum number of concentrations, and the optimal concentrations are often very widely spaced. For transport studies on living cells, we believe that measuring velocities at many concentrations and analyzing the data as outlined here is the most reasonable approach. Substrate solubility and product detection can be important factors influencing the choice of high concentrations for real experiments.

We have described new results for glutamate transport by HeLa and CHO cells and used these results to illustrate a few rarely exploited features of a popular fitting method. Michaelis-Menten parameters provide well-accepted, physiologically relevant descriptions of transport systems and statistical analysis supplies a convenient method for their determination. Some of the considerations described here are likely to be less important when dealing with a purified enzyme *in vitro*, but the benefits obtained by a fuller utilization of the Marquardt method, including checking goodness-of-fit, analyzing parameter distributions, significance testing, and optimizing parameter precisions, will apply to similar complex situations. It is worth repeating the point that these statistical tools are not a substitute for experience, insight and good experimental technique. If velocity measurements are associated with large standard deviations they will fit with acceptable  $q$  values to many different models, but the fits will yield parameters with large standard deviations. When velocities are precisely determined, parameter precision improves and the goodness-of-fit may offer the experimenter impartial guidance in choosing among reasonable models.

Glutamate is a non-essential amino acid and it is,

perhaps, surprising that its transport in mammalian cells is relatively complex. There is clear evidence from other studies that more than one system can be expressed in the same cell [8,10,33]. Our results add further, but interesting, complications. In HeLa, glutamate transport responds rapidly to starvation and this may suggest that some glutamate transporters are subject to regulatory control. Such alterations in glutamate transport have not been reported for other cells. Transport in CHO is stable in the face of starvation, but two saturable systems were initially assumed to be one. It is possible that multiple systems have gone similarly undetected in other studies. Further work will be required to classify and better describe these systems and their novel features in HeLa and CHO.

### Acknowledgements

We want to thank Dr. Glenn Herrick for valuable comments on an early version of this manuscript and Dr. David Mason for helpful discussions of mathematics and statistics. We also benefited from the reviewers' thoughtful criticisms and suggestions. This work was supported by NSF Grant DCB 8904388 to J.F.A.

**Note added in proof** (Received 5 May 1993)

Vol. 210 of *Methods in Enzymology* [34], devoted entirely to numerical calculations in biochemistry, recently appeared and provides additional information on many of the points discussed here.

### References

- Christensen, H.N. (1989) *Methods Enzymol.* 173, 576–616.
- Stein, W.D. (1986) in *Transport and Diffusion across Cell Membranes*, pp. 231–361, Academic Press, San Diego.
- Wilkinson, G.N. (1961) *Biochem. J.* 80, 324–332.
- Cleland, W.W. (1963) *Nature* 198, 463–465.
- Brooks, S.P.J. and Suelter, C.H. (1986) *Int. J. Bio-Med. Comput.* 19, 89–99.
- Kuby, S.A. (1991) *A Study of Enzymes*, Vol. I: Enzyme Catalysis, Kinetics and Substrate Binding, pp. 359–376, CRC Press, Boca Raton.
- Leatherbarrow, R.L. (1990) *Trends Biochem. Sci.* 15, 455–458.
- Lerner, J. (1987) *Comp. Biochem. Physiol.* 87B, 443–457.
- Bannai, S. and Kitamura, E. (1980) *J. Biol. Chem.* 255, 2372–2376.
- Dall'Asta, V., Gazzola, G.C., Franchi-Gazzola, R., Bussolati, O., Longo, N. and Guidotti, G.G. (1983) *J. Biol. Chem.* 258, 6371–6379.
- Puck, T.T., Marcus, P.I. and Ciecuira, S.J. (1956) *J. Exp. Med.* 103, 273–284.
- Pauw, P.G., Sheck, R.N. and Ash, J.F. (1989) *Mol. Cell. Biol.* 9, 116–123.
- Gazzola, G.C., Dall'Asta, V., Franchi-Gazzola, R. and White, M.F. (1981) *Anal. Biochem.* 115, 368–374.
- Smith, P.K., Krohn, R.I., Hermanson, G.T., Mallia, A.K., Gartner, F.H., Provenzano, M.D., Fujimoto, E.K., Goeke, N.M., Olson, B.J. and Klenk, D.C. (1985) *Anal. Biochem.* 150, 76–85.
- Marquardt, D.W. (1963) *J. Soc. Ind. Appl. Math.* 11, 431–441.
- Press, W.H., Flannery, B.P., Teukolsky, S.A. and Vetterling, W.T. (1988) in *Numerical Recipes in C: The Art of Scientific Computing*, pp. 216–565, Cambridge University Press, New York.
- Shapiro, S.S. and Wilk, M.B. (1965) *Biometrika* 52, 591–611.
- Royston, J.P. (1982) *Appl. Stat.* 31, 176–180.
- Motulsky, H.J. and Ransnas, L.A. (1987) *FASEB J.* 1, 365–374.
- Finkelstein, M.C., Slayman, C.W. and Adelberg, E.A. (1977) *Proc. Natl. Acad. Sci. USA* 74, 4549–4551.
- Franchi-Gazzola, R., Gazzola, G.C., Dall'Asta, V. and Guidotti, G.G. (1982) *J. Biol. Chem.* 257, 9582–9587.
- Fairgrieve, M., Mullin, J.M., Dantzig, A.H., Slayman, C.W. and Adelberg, E.A. (1987) *Somat. Cell Mol. Genet.* 13, 505–512.
- Nicholls, D. and Atwell, D. (1990) *Trends Pharmacol. Sci.* 11, 462–468.
- Cleland, W.W. (1967) *Adv. Enzymol.* 29, 1–32.
- Mannervik, B. (1982) *Methods Enzymol.* 87, 370–390.
- Cornish-Bowden, A. and Endrenyi, L. (1981) *Biochem. J.* 193, 1005–1008.
- Allison, R.D. and Purich, D.L. (1979) *Methods Enzymol.* 63, 3–22.
- Weber, G. (1965) in *Molecular Biophysics* (Pullman, B. and Weissbluth, M., eds.), pp. 369–396, Academic Press, New York.
- Deranleau, D.A. (1969) *J. Am. Chem. Soc.* 91, 4044–4049.
- Deranleau, D.A. (1969) *J. Am. Chem. Soc.* 91, 4050–4054.
- Endrenyi, L. (1981) in *Kinetic Data Analysis* (Endrenyi, L., ed.), pp. 137–167, Plenum Press, New York.
- Duggleby, R.G. (1981) in *Kinetic Data Analysis* (Endrenyi, L., ed.), pp. 169–179, Plenum Press, New York.
- Christensen, H.N. (1990) *Physiol. Rev.* 70, 43–77.
- Brand, L. and Johnson, M.L. (eds.) (1992) *Numerical Computer Methods, Methods in Enzymology*, Vol. 210, 718 pp., Academic Press, San Diego.